Communicating Research to the General Public

At the March 5, 2010 UW-Madison Chemistry Department Colloquium, the director of the Wisconsin Initiative for Science Literacy (WISL) encouraged all Ph.D. chemistry candidates to include a chapter in their Ph.D. thesis communicating their research to non-specialists. The goal is to explain the candidate's scholarly research and its significance to a wider audience that includes family members, friends, civic groups, newspaper reporters, state legislators, and members of the U.S. Congress.

Ten Ph.D. degree recipients have successfully completed their theses and included such a chapter, less than a year after the program was first announced; each was awarded $500.

WISL will continue to encourage Ph.D. chemistry students to share the joy of their discoveries with non-specialists and also will assist in the public dissemination of these scholarly contributions. WISL is now seeking funding for additional awards.

Wisconsin Initiative for Science Literacy

The dual mission of the Wisconsin Initiative for Science Literacy is to promote literacy in science, mathematics and technology among the general public and to attract future generations to careers in research, teaching and public service.

UW-Madison Department of Chemistry
1101 University Avenue
Madison, WI 53706-1396
Contact: Prof. Bassam Z. Shakhashiri
bassam@chem.wisc.edu
www.scifun.org

January 2011

DYNAMICS OF RNA POLYMERASE AND DNA FOCI IN LIVE *ESCHERICHIA COLI*

by

BENJAMIN PAUL BRATTON

A dissertation submitted in partial fulfillment of the

requirements for the degree of

Doctor of Philosophy

(Chemistry)

at

THE UNIVERSITY OF WISCONSIN-MADISON

2011

Chapter 2 — Tracking *oriC* diffusion with biplane imaging

2.1 Introduction

One of my projects during graduate school was attempting to answer the question "How rapidly does a piece of DNA move around inside a bacterial cell." The specific piece of DNA of interest was the origin of chromosomal replication, *oriC*. Determining how rapidly a piece of DNA is able to move about in the cell is a fundamental science question. That is, it attempts to understand the underlying physical principles that govern how the natural world works. While my thesis work did not involve inventing a new way of killing bacteria or understanding how they develop antibiotic resistance, it does add to the wealth of knowledge of understanding the physical world. Even though *E. coli* are widely studied and extremely well known, there are still many aspects of their internal structure and dynamics to be explored. This chapter briefly discusses diffusion and its importance in bacterial cells, the experimental technique for measuring diffusion and some of the data from the project.

In an *E. coli* cell, the genetic information is in a single circular chromosome, roughly 1.5 mm in length. As a cell grows and gets ready to divide, it replicates its DNA. Replication is the process of making two identical copies of the chromosome, one for each of the daughter cells. Because the *E. coli* chromosome is circular, the cell needs a way to initiate and terminate replication, ensuring that the entire chromosome is copied at one time. In a similar fashion, if one were to make a copy of all of the contacts from someone's Rolodex, he would want to make sure that he started and ended in known locations, not wasting his energy by copying the same contact

multiple times. In the Rolodex example, one may start at the letter A and stop after Z. For replication in *E. coli*, the cell starts at the origin, called *oriC*, and proceeds simultaneously in both directions until reaching the terminus, called *ter*.

2.2 Diffusion and a game of coin flips

Living cells are, in many ways, like small factories. They bring in raw materials from the outside world, make new products based on some instruction set, use the finished products for some purpose and deal with the waste created along the way. Through all of these processes in a large factory, there is a regulated and specific path for every type of material. In large eukaryotic cells (plant, animal and fungus), this type of directed, active transport is used to ensure that large cargos reach their destinations. However, for small prokaryotic cells (bacteria, archea), the cells are usually able to depend on diffusion to keep the contents mixed. Diffusion uses the random fluctuations of the solution to mix and redistribute content. As described below, the time required for diffusion to move cargo is related to the square of the distance that it needs to move. For small bacterial cells, this is not a problem and the cell does not need to spend energy moving cargo from one place to another. For large eukaryotic cells, they spend energy to ensure that the cargo goes where it is needed in an expedient fashion.

To better understand the distance squared nature of diffusion, it may be helpful to look at a specific example. This example is often referred to as the walk of the drunken sailor (1), but I will describe it in slightly different terms. Imagine that a token is in very simple maze, a number line (Figure 2.1). Each turn, it moves exactly one unit in any direction as determined by the flip of a coin. Heads, move it to the left, tails, to the right. If the number line had three dimensions,

its motion would depend on the roll of a die. Rolling a one moves it forward, a six moves it back, two moves it up, etc. To play the game, one bets on the number of turns it will take to get the token out of the maze. Granted, this may be quite a boring game, but the question is how to make an intelligent wager.

If the line went from 1 to 5 and the game starts at 3, the fastest way to leave would be to move right to 4, right to 5 and right Out. It would also be just as efficient to move left to 2, left to 1 and left Out. While these are the fastest ways to leave, they are not very likely to occur. First, look at the outcomes possible after a certain number of flips of the coin (Figure 2.1). After one flip, the token could be at 2 or at 4 and assuming a fair coin, it has a 50% chance of being at either. After the second flip, it is at 1, 3 or 5. Because the coin is fair, average distance traveled after each coin toss is 0. That means that on average, the token never moves. This is a misleading statement because it is obvious that eventually the token will move off the number line. The key to the game is to look at the square of the distance travelled away from the center. After one flip, the average or mean squared distance (MSD) is 1 unit. After two flips, the MSD is 2.

$$\frac{4(HH)+0(HT)+0(TH)+4(TT)}{4}=2 \qquad \textbf{Eq. 2.1}$$

After three flips, the MSD is 3.

$$\frac{9(HHH)+6(HHT,HTH,HTT,THH,TTH,THT)+9(TTT)}{8}=2 \qquad \textbf{Eq. 2.2}$$

Clearly, the MSD scales linearly with the number of flips. So, when playing this coin flipping game, one should bet based on the square of the number of units that she anticipates needing to move.

Now, if one were playing this game with two tokens, an interesting question to ask would be, "what if each token moves with different step size?" That is, if two tokens have the same size maze but one takes steps of size two instead of one, how many fewer steps will that token need to take? Using the same strategy as discussed above, after two flips, the MSD would be 8, and after three steps, 12.

$$\frac{16(HH)+0(HT)+0(TH)+16(TT)}{4}=8 \qquad \textbf{Eq. 2.3}$$

$$\frac{36(HHH)+6\cdot 4(HHT,HTH,HTT,THH,TTH,THT)+36(TTT)}{8}=8 \qquad \textbf{Eq. 2.4}$$

Following the same thought process with a step size of three yields a two-step MSD of 18 and a three-step MSD of 27. The MSD follows a simple formula as a function of the step size *s* and the number of steps *n*

$$MSD(s,n)=s^2\cdot n \qquad \textbf{Eq. 2.5}$$

While it seems unlikely that a game of this kind will sweep the nation's casinos, it helps to illustrate how diffusion works. Diffusion of single particles behaves in exactly the same way as the token moving along the number line. If one is able to measure the MSD as a function of time, one can determine the effective size of the steps, *s*. This is exactly the goal of my research, determining the effective step size *s* by measuring MSD as a function of time. The size s^2 in diffusion is called the diffusion constant and, as this example shows, has units of length^2 per time step. In the systems that I explored during my graduate career, the unit of length that made the most sense was the micron, μm, 1/1000th of mm long. The most appropriate unit of time was the second. I reported diffusion constants in units of $\mu m^2\ s^{-1}$. Unlike the one-dimensional maze

described above, *oriC* moved and was measured in in three dimensions, *xy* and *z*. Section 2.3 describes how the *xy* and *z* positions were determined.

2.3 Single particle tracking and biplane imaging

For the coin flipping game, it was easy to determine the position of the token, it could only occupy integers on the number line. When measuring the diffusion of *oriC*, it was not so simple. We obtained a bacterial strain from Tamas Gaal in the Department of Bacteriology, UW-Madison. This strain contained green fluorescent protein (GFP) tagged to a DNA binding protein called ParB. ParB naturally binds to *parS*, so Tamas placed a copy of *parS* near *oriC*. The combination of the two resulted in a bright, fluorescent spot at each copy of *oriC* in the cell. To photograph these bright spots, we used an inverted fluorescence microscope (Nikon, TI-E) with a $100\times$ phase contrast objective and an argon ion laser (488 nm, Melles Griot 532-AP-A01) as a light source. Images were captured by a low light, electron multiplying charge coupled device (EMCCD) (Andor Technologies, iXon DV-897), which is basically a $35,000 digital camera. This enabled us to take pictures of the *E. coli* with brightly labeled *oriC* at 10 frames per second. As shown in Figure 2.2, the bacterial cells look like small capsules or spherocylinders and have dim background fluorescence. The cells are about 1 μm in diameter and 3 μm long. Each copy of *oriC* appears as a bright spot above the dim background fluorescence. We filtered the images (3, 6, 7) to remove the background fluorescence, leaving bright peaks on a dark background (see Figure 2.2). From this image, a small box was drawn around each spot. The (*row*, *col*) position of each spot was determined as the center of mass of this sub-image.

The *z* position of the spot was determined using a biplane imaging. To explain the concept of biplane imaging, one should imagine taking a picture of a simple object. One such example is shown in Figure 2.3. If a camera with a fixed focal length is positioned to take a picture of the object, moving either the object or the camera will cause it to go out of focus. Moving both the camera and the object will leave the object in focus. Figure 2.4 shows an image where different objects are differentially out of focus. From one single image, it is not possible to tell the distance between the lines of the eye chart. The fourth and fifth lines are blurred by the same amount, but it is not clear if they are closer or further away from the camera. By taking a second image with the camera focused at another position, we can determine that the fourth line was closer to the camera and the fifth line was further away. Determining the absolute position of each of the lines in the eye chart requires a calibration of camera blur.

When measuring dynamics in live biological samples, it is not possible to refocus the microscope and take a second image of the same sample. In the time that it takes to focus to a different position, the sample will already have moved. For this reason, we used the work of the Bewersdorf lab (2, 4) and built a device that allows a single camera to look at two focal planes in the sample at the same time. Figure 2.5 shows an illustration of how the calibration of this device was performed. A stationary sample of 27 nm diameter, bright fluorescent beads was placed on the microscope. The microscope objective was moved closer to the sample in 100 nm increments. This effectively moves the focal plane of the microscope up toward the sample in 100 nm increments. At each position of the objective, images of the beads from two focal planes were recorded separately on two channels of the camera. As can be seen in Figure 2.6, as the bead came into focus, it appeared bright and sharp. As it went out of focus, it became dimmer

and blurry. Because the focal planes of the biplane device are different, the bead appeared in focus for a different height of the objective.

To quantify the blurriness of the image, we calculated the Brenner gradient of the image for each camera channel (3). As shown in Figure 2.7, the Brenner gradient compares an image with a shifted version of itself. If the object is in focus, the Brenner gradient is large because there is a clear difference between the original and shifted images. If the object is blurred and out of focus, the Brenner gradient is small because the shifted image is very similar to the original.

2.4 Results

Using the calibration determined above, we measured the *z* position of *oriC* in live *E. coli*. Once we had the (*row*, *col*, *z*) coordinates of each copy of *oriC*, we rotated and centered each cell. This enabled us to separate movements along the long axis of the cell *x*, the short axis of the cell *y* and the focal axis of the microscope *z*. From these *xyz* we grouped the positions from the same copy of *oriC* into a trajectory and calculated the mean squared displacement (*MSD*) as a function of time between the measurements (τ). Figure 2.8 illustrates how this mean squared displacement was calculated from a trajectory. First, the length of each of the 1-step displacements was calculated. These were the distances between the particle in each frame and the subsequent frame. In Figure 2.8, these are marked in black bars. The average of the square of these distances was recorded as $MSD(\tau=1)$. In a similar fashion the 2-step displacements were the distance between the positions in one frame and two frames later. The 2-step displacements are shown in Figure 2.8 in red and the 3-step displacements are shown in blue.

Figure 2.9 shows the *MSD*(τ) separated into the three dimensions *xyz*. The shape of *MSD*(τ) is determined by the underlying dynamics. For this dataset, the dynamics were more complicated than the simple diffusion illustrated in the coin flipping example. That example had an MSD that scaled linearly with the number of steps. On a plot of *MSD*(τ), this would have been a straight line. The dynamics in our dataset were clearly non-linear. The very rapid dynamics of our dataset, $\tau<0.75$ s, appeared like diffusion with a relatively large diffusion constant ($3\text{-}5\times 10^{-3}$ $\mu m^2 s^{-1}$), however *oriC* appeared confined in a 160 nm domain. This confinement meant that *oriC* could not get infinitely from where it started. This caused a bending over in *MSD*(τ), clearly visible by about 0.75 s. At longer time lags, *MSD*(τ) is again linear, albeit with a reduced diffusion constant of 0.3×10^{-3} $\mu m^2 s^{-1}$.

The difference in *MSD*(0) between *x*-*y* and *z* shows the lack of precision in the *z* dimension relative to *x*-*y* (Figure 2.9). Multiple measurements of the position of a stationary bead had a standard deviation of 25 nm in *x*-*y* and 95 nm in *z*. After removing the difference in *MSD*(0), the *y*-*z* dimensions appeared to have similar dynamics. The *x* dimension was slightly less confined but the overall shape of the curve was similar. The stronger confinement in the *y*-*z* dimension is consistent with a model of the *E. coli* chromosome being squeezed more tightly in the radially dimension of the cell than along the axis of the cell (5).

2.5 Acknowledgements

This project would not have been possible without Renée Dalrymple and Tamas Gaal. Renée and I worked together on the experimental design and data collection in this project and Tamas Gaal provided the bacterial strains necessary. Sample preparation, image collection and

data analysis were performed in the lab of James Weisshaar. Funding and support for this project were provided by NIH grants R01 R01GM086468 an ARRA award and R21NS062233. BPB was supported in part by NIH training grant T32GM008293.

2.6 References

1. **Berg, H. C.** 1993. Random Walks in Biology. Princeton University Press, Princeton, N.J.

2. **Bolduc, S., and S. Hess** Bi-Plane FPALM - Senior Project 2009-2010. http://sites.google.com/site/biplanefpalm/home [Online.]

3. **Brenner, J. F., B. S. Dew, J. B. Horton, T. King, P. W. Neurath, and W. D. Selles.** 1976. An automated microscope for cytologic research a preliminary evaluation. Journal of Histochemistry & Cytochemistry **24:**100-111.

4. **Mlodzianoski, M. J., M. F. Juette, G. L. Beane, and J. Bewersdorf.** 2009. Experimental characterization of 3D localization techniques for particle-tracking and super-resolution microscopy. Optics Express **17:**8264-8277.

5. **Mondal, J., B. P. Bratton, Y. Li, A. Yethiraj, and J. C. Weisshaar.** 2011. Entropy-Based Mechanism of Ribosome-Nucleoid Segregation in E. coli Cells. Biophysical Journal **100:**2605-2613.

2.7 Figures

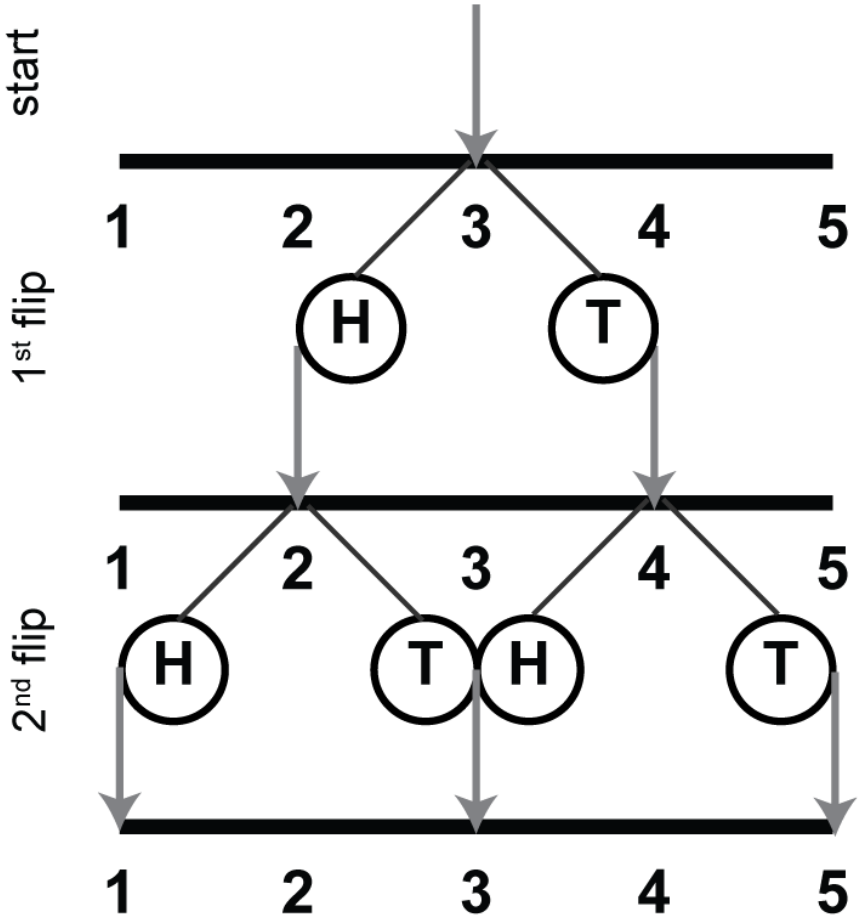

Figure 2.1. Example coin flipping game.

In this game, the token is moved exactly one space after each flip, either one unit to the left with the toss of a heads, or one unit to the right with the toss of a tails. Wagers are placed on the number of flips required to move the token out of the maze. Like diffusion, the average number of flips grows with the square of the distance to travel.

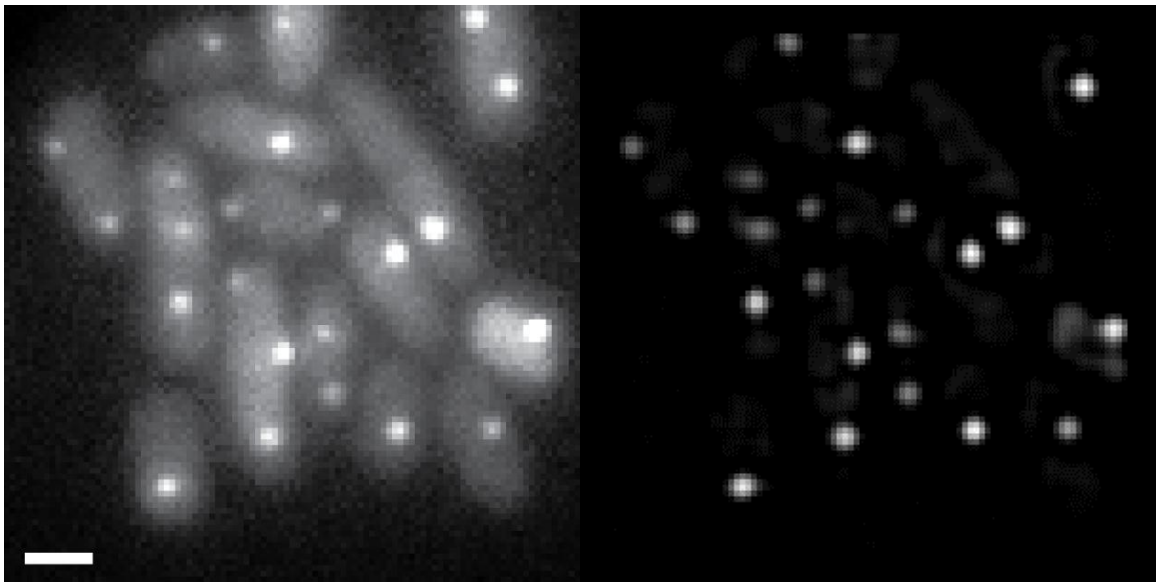

Figure 2.2. Fluorescence image of *E. coli* with *oriC* tagged with green fluorescent protein.

Scale bar is 1/1000th mm or 1 µm. (*left*) before and (*right*) after application of a spatial bandpass filter to remove the background fluorescence and enable easy detection of the peaks.

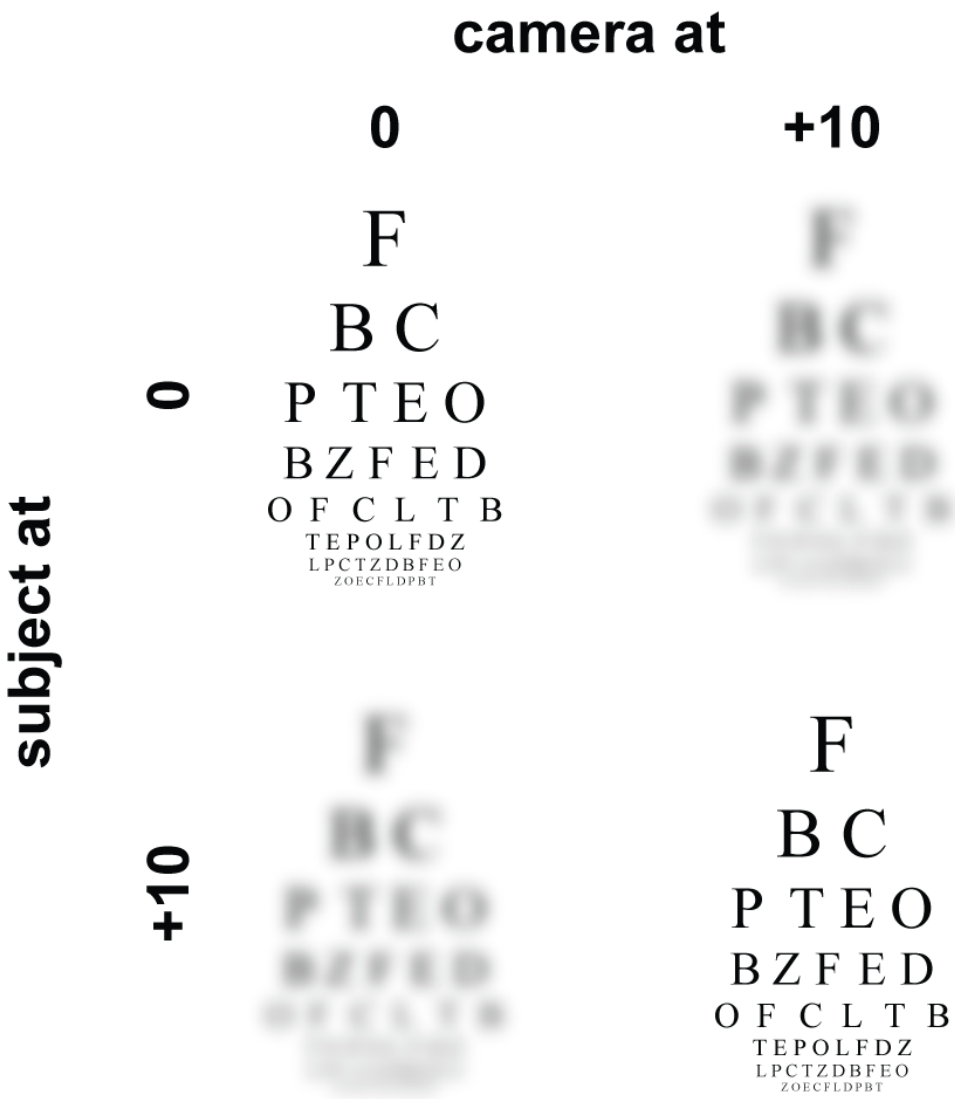

Figure 2.3. Illustration of the blurring of a photograph induced by moving the subject or the position of the fixed focal length camera.

(Upper left, bottom right) If the object and the camera are both moved together, the image remains in focus. (Upper right, bottom left) If just the subject or just the camera is moved, the image appears blurry. The level of blurriness depends on the relative distance between the camera and subject. Eye chart letter ordering from http://www.i-see.org.

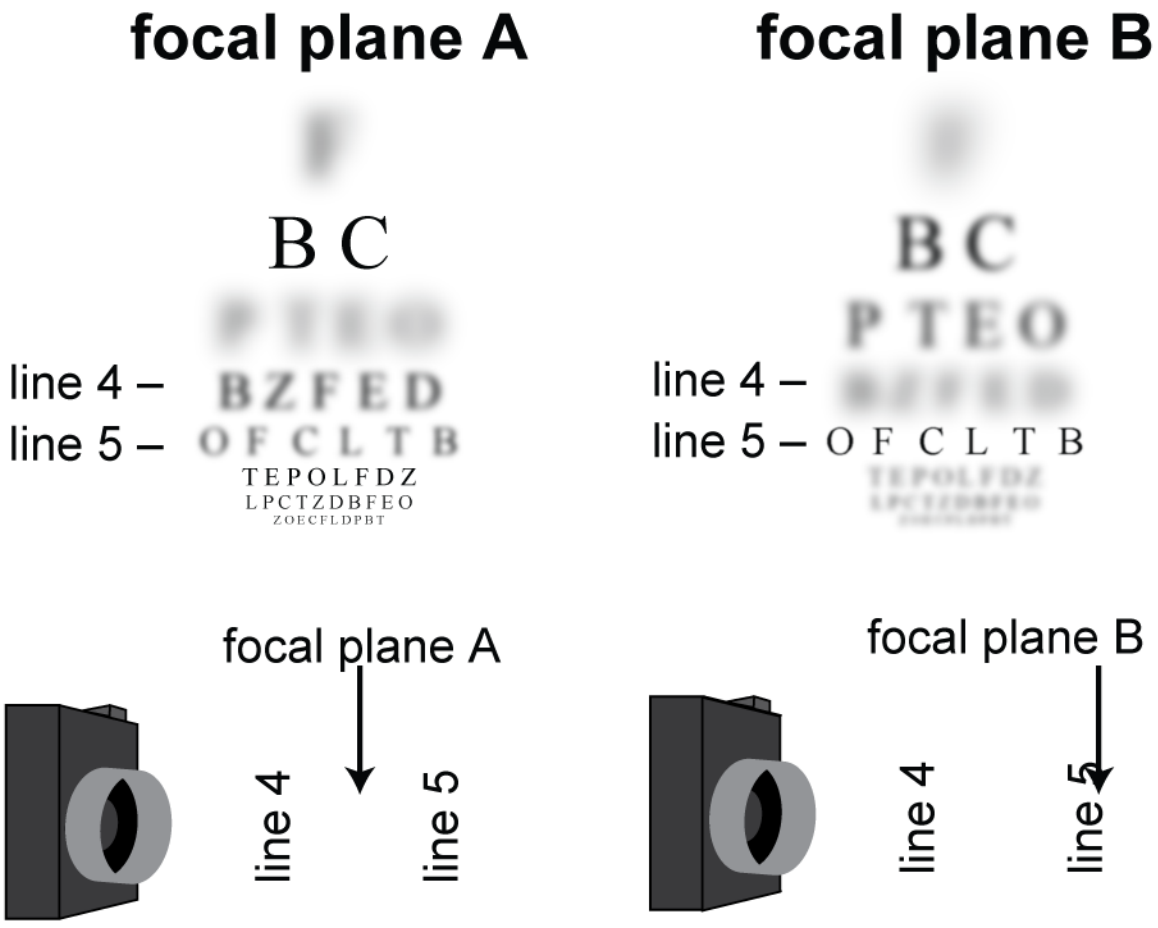

Figure 2.4. Illustration of biplane imaging.

If each line of the eye chart is at a different distance from the camera, focusing on one plane shows lines of differing blurriness. At least two focal planes must be photographed to determine the positions of the subjects. Although lines 4 and 5 are equally blurry in focal plane A, focal plane B shows that line 4 was out of focus closer to the camera and line 5 was out of focus further from the camera. Eye chart letter ordering from http://www.i-see.org.

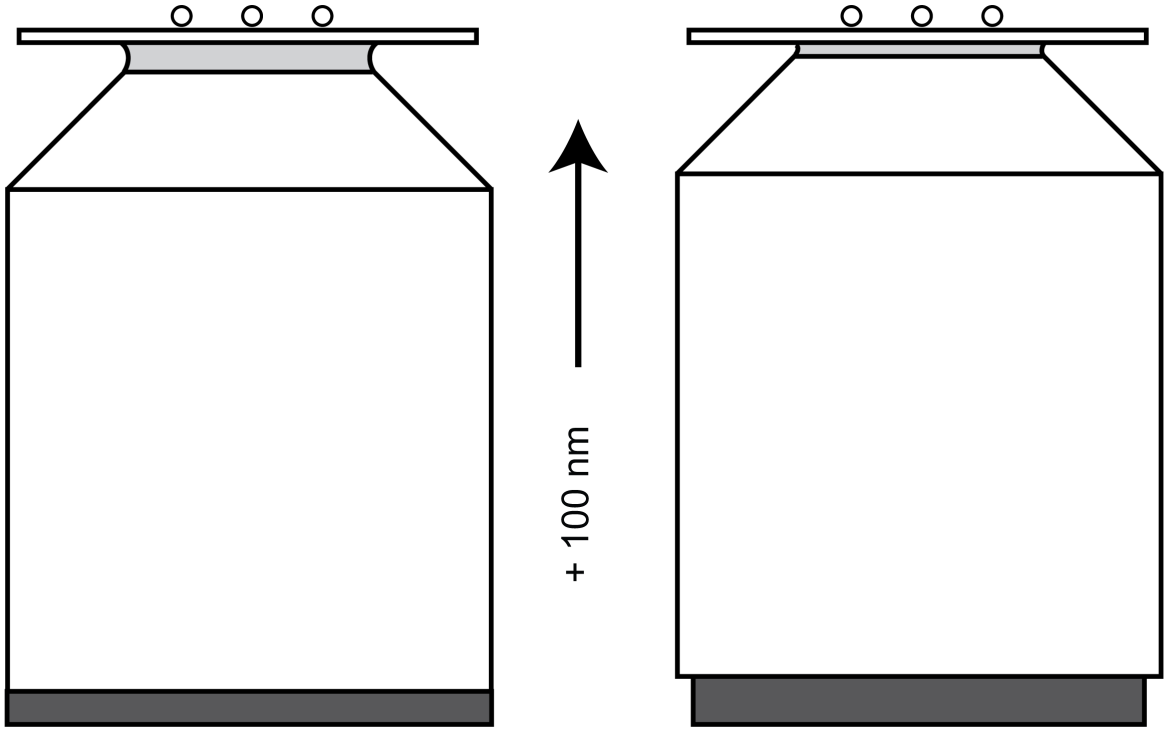

Figure 2.5. Calibration images are taken by moving the objective progressively closer to the sample.

This diagram illustrates raising the objective by a piezo device (dark gray). Because the 27 nm bead sample is held in place, this moves the objective further into the immersion oil (light gray) and decreases the distance between the objective and at the sample. Effectively, this forces the microscope to focus at a higher focal plane. Elements in the illustration are not to scale.

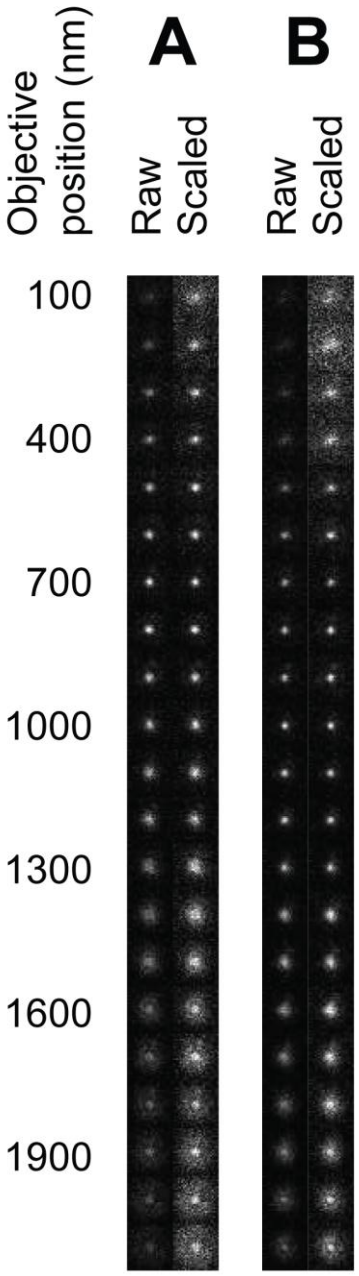

Figure 2.6. Example calibration images of 27 nm fluorescent beads taken in 100 nm increments. Images of the bead in (A) the top half and (B) the bottom half of the camera. Raw images show the change in intensity as a function of height and scaled images show the change in clarity as a function of height.

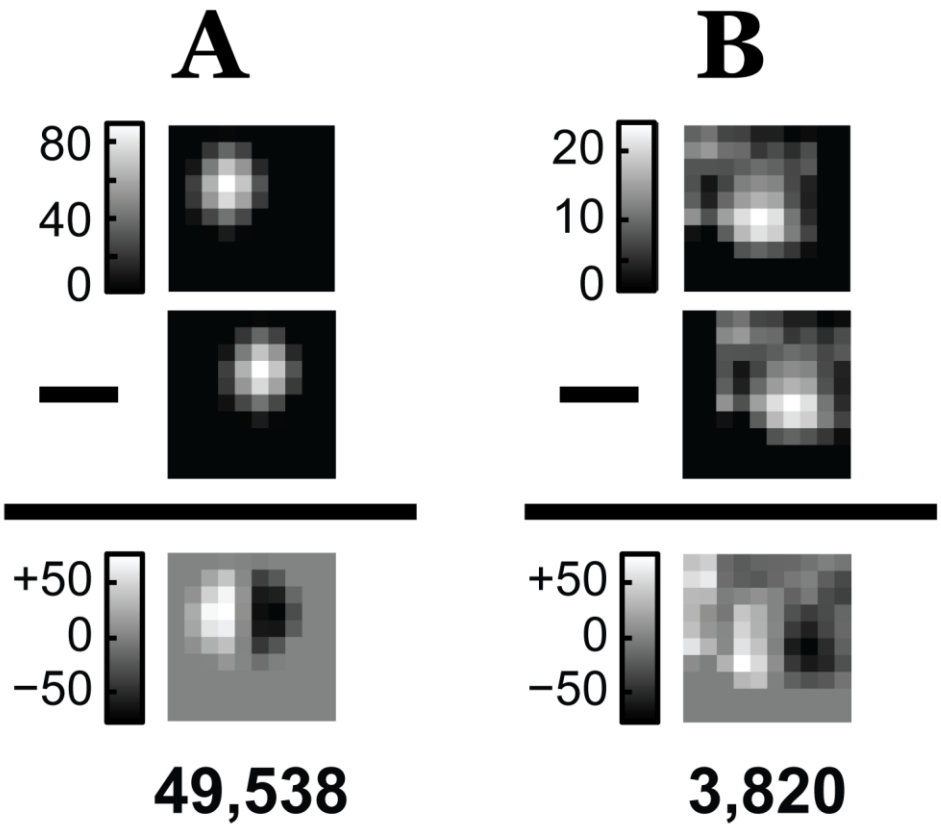

Figure 2.7. The Brenner gradient is determined by calculating the sum of the squared difference between the image and a shifted version of itself. Here the image is of a 27 nm fluorescent bead. (A) When the image is in focus, the difference is large and the Brenner gradient is large. (B) When the image is out of focus, the difference and Brenner gradient are near 0. The value of the Brenner gradient for each image, the sum of the squared differences, is displayed below the difference image.

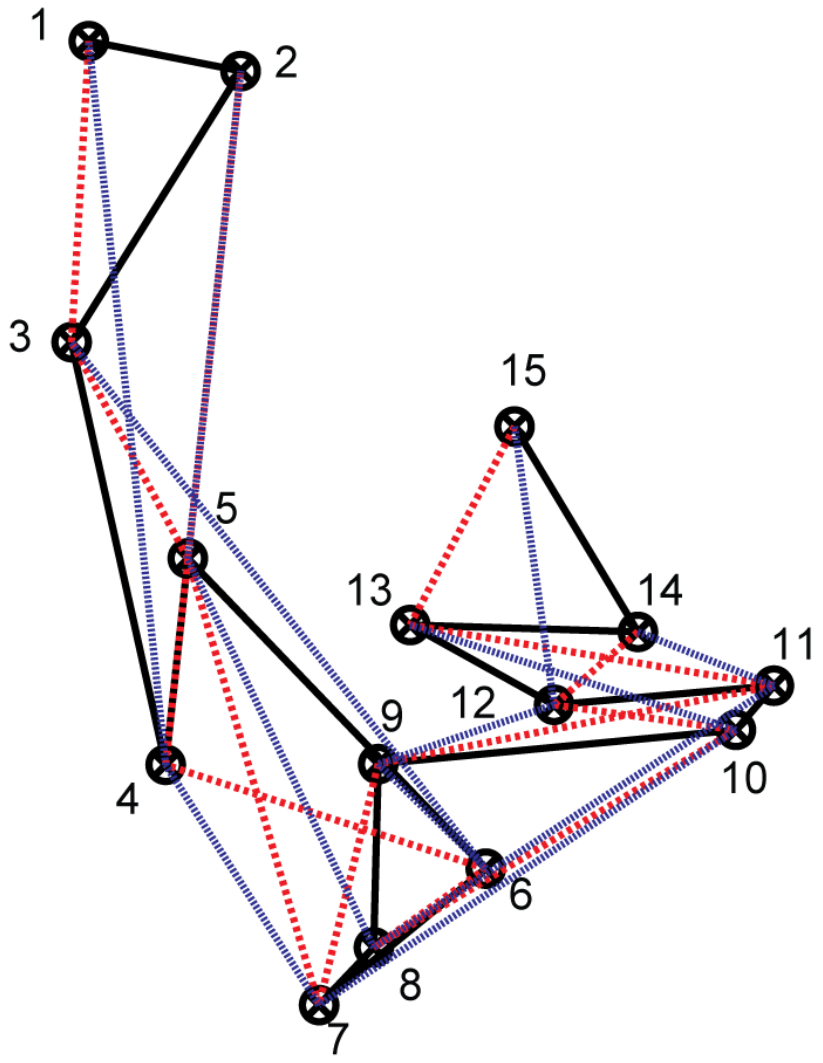

Figure 2.8. Illustration of calculating the mean squared displacement as a function of time lags *MSD*(*τ*)

1-step displacements are shown in black, 2-step displacements are shown in red and 3-step displacements are shown in blue.

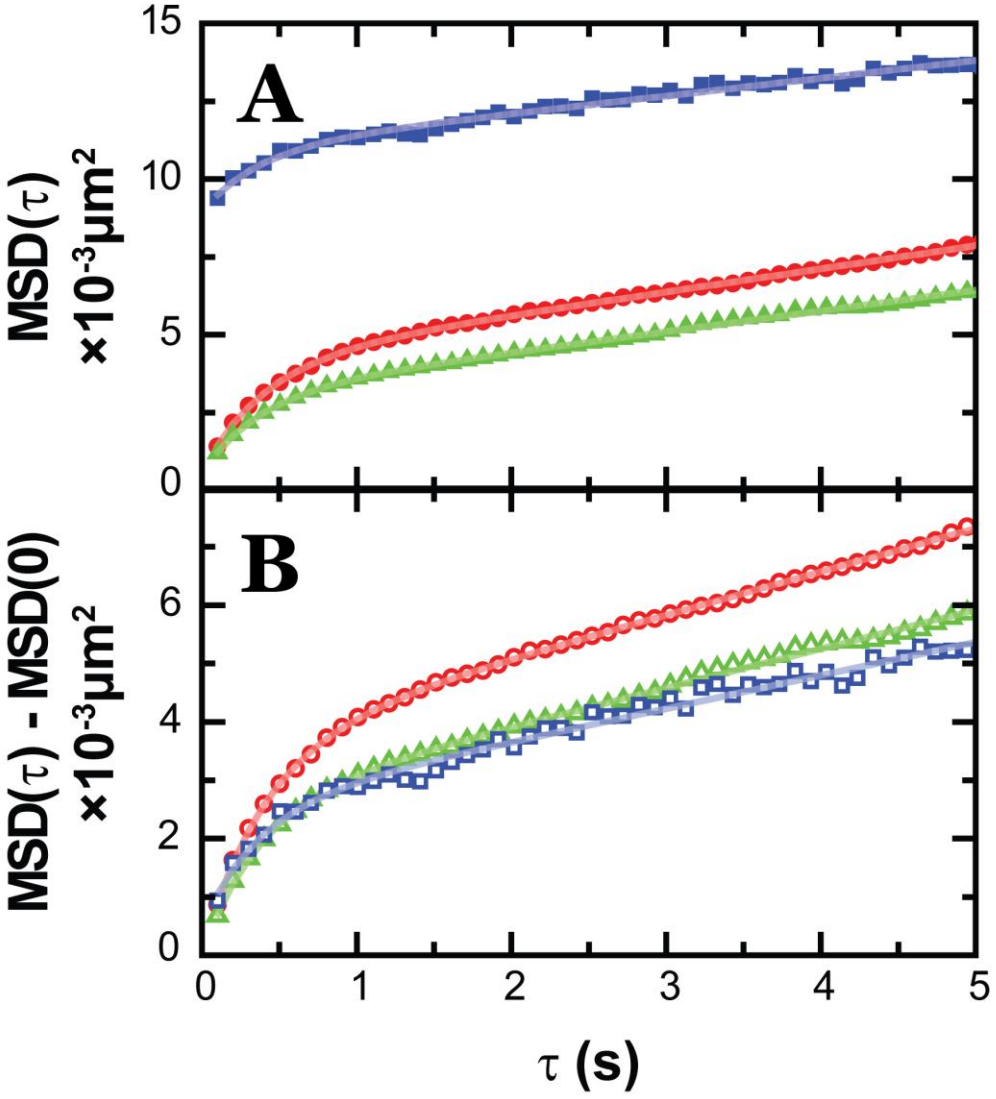

Figure 2.9. Mean squared displacement of *oriC* along single dimensions up to time lags of 5 s. Displacements along x are in red circles, along y are in green triangles and along *z* are in blue squares. (A) Data are plotted on an absolute scale, showing the difference in offset between *xy* and *z*. (B) Data are shifted so that their offsets are equal to zero.